ARMA 17-411

Use of Seismic Wave Conversions (S-to-P wave) to Monitor Shear Crack Growth

Modiriasari, A.
Lyles School of Civil Engineering, Purdue University, West Lafayette, IN, USA
Bobet, A.
Lyles School of Civil Engineering, Purdue University, West Lafayette, IN, USA
Pyrak-Nolte, L.J.
Department of Physics and Astronomy, Department of Earth and Atmospheric Sciences, Lyles School of Civil Engineering, Purdue University, West Lafayette, IN, USA

ABSTRACT: In the laboratory, uniaxial compression experiments were performed on prismatic specimens of Indiana limestone with two pre-existing parallel flaws. Full waveform measurements of shear waves were used to monitor shear crack initiation and propagation in rock. Simultaneously, digital image correlation (DIC) was used to monitor the damage evolution on the specimen surface by measuring full-field displacements. The shear cracks that initiated from the flaws tips that ultimately produced coalescence were observed to propagate roughly parallel to the loading direction such that the waves impinged on the crack plane at normal incidence. The amplitude of the transmitted waves did not change significantly with shear crack initiation. However, shear to compressional wave conversions occurred when a shear crack was initiated, roughly at 76% of the load detected with DIC. The wave conversion is associated with micro-cracks generated as the shear crack initiates. The amplitude of the converted waves increased with shear crack growth and reached a maximum at coalescence. Observation of converted waves provides a means for monitoring shear cracks, given that past research has shown that transmitted waves were not sensitive to shear crack initiation.

1. INTRODUCTION

Discontinuities play an important role in the behavior and stability of the rock mass, as well as in the flow of fluids through the rock. Discontinuities occur on different scales, from micro-cracks to fractures and faults. Given the role that pre-existing and induced discontinuities have in rock mass behavior, it is critical to develop techniques that can be used to identify and characterize fractures inside the rock, as well as their evolution with stress changes or with time.

Several investigators have shown that seismic methods can be used to monitor or even predict rock mass behavior. They have shown that local and microscopic changes of the physical properties of the rock matrix and of the discontinuities affect seismic characteristics such as amplitude and velocity (Pyrak-Nolte et al., 1990, Chen et al., 1993, Pyrak-Nolte, 1996, Nakagawa et al., 2000, Kahraman, 2002, Leucci and De Giorgi, 2006, Shao and Pyrak-Nolte, 2013, Byun et al., 2015). Transmitted and reflected compressional (P) and shear (S) waves have been used in our previous work to identify the evolution of tensile and shear cracks inside the rock. The experimental results consistently show that changes in the amplitudes of transmitted seismic waves can be used for detection of damage evolution in the form of tensile cracks, but cannot identify the initiation of shear cracks (Modiriasari et al., 2015).

In addition to changes in amplitude of transmitted and reflected P- and S-waves, seismic wave conversions, e.g. from S- to P- or P- to S-waves, offer the possibility of further exploring the response of fractures under load. Theoretical considerations, supported by laboratory experiments, show that obliquely incident P- and S-waves impinging on a fracture generate converted S- and P-waves, respectively (Aki et al., 1982, Gu et al., 1996, Nakagawa, 1998, Nakagawa et al., 2000). This occurs for both welded and non-welded interfaces. Nakagawa et al. (2000) showed experimentally and theoretically that P to S (also S to P) converted modes occur even when the incident wave is normal to a fracture. They observed P-to-S converted modes on a fracture undergoing dilation during shearing. In their study, the fracture was idealized as small random asperities superposed on regular saw-tooth profiles. As the fracture was sheared and dilation occurred, openings between the asperities were created that had a preferred orientation parallel to one of the sides of the saw-tooth asperities. This array of inclined open flat cracks induces a coupled response, as a normal stress applied to the fracture results in shear displacement across the fracture and a shear stress is accompanied by normal displacement. Such behavior was incorporated into the displacement discontinuity theory (Pyrak-Nolte et al., 1990, Pyrak-Nolte, 1996) by including cross-coupling fracture specific stiffness. Nakagawa et al. (2000) linked the coupling stiffness of fracture to the occurrence of converted waves. As the coupled stiffness increases, wave conversion increases.

Nakagawa et al. (2000) suggested that shear-induced conversion of seismic waves could be used for detecting and measuring the shear stress acting on a fracture. They observed that the amplitude of the converted waves increased with the shear stress applied to the fracture. In addition, the direction of the shear stress could be determined, as the phase of the particle motions of the converted waves change with the direction of shear. While the previous studies suggest that wave conversion could be used as a diagnostic tool for examining the shear stress on a fracture, it is not clear whether S-to-P or P-to-S converted modes can be utilized to detect the onset of shear crack formation.

In this paper, we present experimental evidence of a wave conversion signature indicating the initiation of shear cracks long before a macroscopic shear crack is observed in rock. This seismic signature consists of the emergence of a converted mode as S-waves impinge the plane of the incipient shear crack. In addition, we present data that suggest that the seismic waves also contain information about the shear crack growth, crack coalescence, as well as the location of the new crack.

2. LABORATORY EXPERIMENTS

Several prismatic specimens of Indiana limestone were tested under uniaxial compression to investigate seismic precursors to shear crack initiation. The dimensions of the specimens were 203.2 mm in height, 101.6 mm in width, and 38.1 mm in thickness (Fig. 1). Initial measurements of mechanical and physical properties of Indiana limestone were made on intact samples. The average density of the specimens was 2,326 kg/m^3. The Indiana limestone samples had a porosity of 15-25%, unconfined compressive strength (UCS) of 47 MPa, and Young's modulus of 7.4 GPa. P- and S-wave velocities measured in the intact material were 4,380 and 2,570 m/s, respectively.

Two parallel through-going flaws were created perpendicular to the thickness of the specimen using a scroll saw with a 3/4 mm thick blade. The aperture of the flaws was roughly 1mm. The length of the flaws (L) was 19.05 mm. In Fig. 1, the geometry of the flaws is defined with the spacing (S) between the flaws, continuity (C), and inclination angle (β). In this paper, representative data from sample L63 are presented, which had a spacing S=9.525 mm, continuity C=19.05 mm and inclination angle β=60^0. The geometry was associated with coalescence through a shear crack that was produced by the propagation of two shear cracks, each initiation from the internal tips of the flaws. Repeatability tests were done on four more experiments with the same geometry and the results of all the tests were consistent.

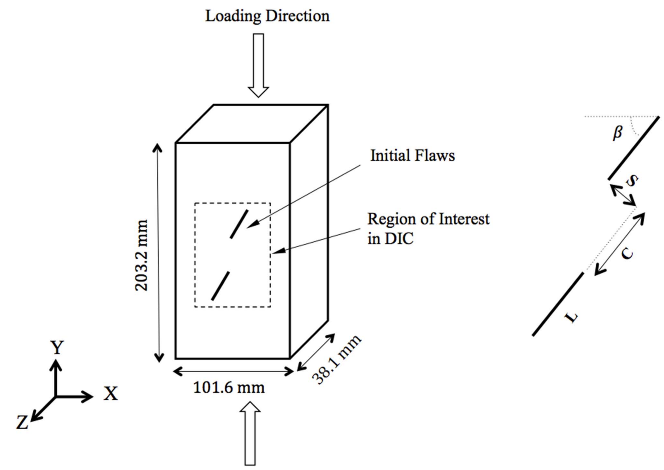

Fig. 1. Schematic of the specimen and flaws used in the experiments

Two steel platens and four springs were used to attach five piezoelectric transducers (central frequency of 1 MHz) to the two sides of the specimen, which were used for sending and receiving seismic waves. The experimental set-up is shown in Fig. 2. A compression of 70 kPa was provided to the side platens through four springs, to hold the transducers in place. The transducers were coupled to the specimen surface with honey. The source transducers were excited with a 400 V square pulse, sent from a high-voltage pulse generator, with a repetition rate of 5 kHz. Five pairs of transducers, i.e. five sources and five receivers, were placed on each side of the specimen. Two pairs of transducers (one pair of Panametrics V103RM for P-waves, and one pair of V153RM for S-waves) were aligned with the external flaw tips to monitor tensile crack initiation and propagation. Another pair of transducers (denoted as 3S in Fig. 2) was placed between the two flaws and was used to monitor the initiation and propagation of the shear cracks at the internal tips of the flaws and also cracks coalescence. The shear wave transducer 3S was polarized vertically along the loading direction. The remaining transducers were placed at higher distances from the flaws tips to monitor changes in the intact material with the loading.

The displacements on the front surface of the specimen (63.5 by 50.8 mm gray square in Fig. 2) were monitored during loading using 2D-DIC imaging. The gray region in the figure is the region of interest (ROI) for the DIC analysis and consisted of a random speckle pattern. As shown in Fig. 2, the ROI was selected to include all the tips of the flaws where the new cracks would initiate during loading. DIC images were recorded using a Grasshopper (Point Grey) CCD camera with 2448x2048 square pixels and a 50 mm focal length lens (model HF50SA1 Fujinon).

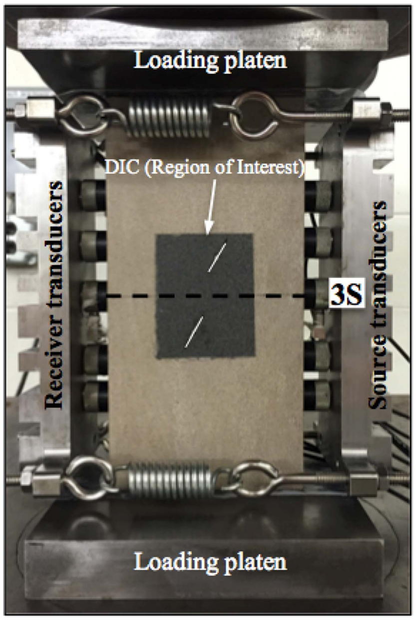

Fig. 2. Experimental set-up

The specimen with the attached transducers and side platens was placed between the platens of an Instron loading machine. A Teflon film was attached to the top and bottom platens using a thin layer of petroleum jelly. This provided stress uniformity and reduced the potential concentration of stresses at the top and bottom surfaces of the specimen. Before any measurements were conducted, the specimen was loaded to 2 MPa uniaxial compression for four hours. This was done to ensure good coupling between the transducers, the honey and the specimen surface, and to minimize changes in the waveforms of the signals. The uniaxial compression load was applied to the specimen at a constant displacement rate of 0.04 mm/min. The load was increased until failure.

During loading, the DIC images were taken at a rate of 2 frames/sec. Simultaneously, transmitted and reflected signals through the specimen were continuously recorded. The load and displacement applied to the specimen were automatically measured every second using a load cell (with a ±445 Newtons average resolution) and Linear Variable Displacement Transducer (LVDT, with 0.5 micron resolution) on the loading machine. The load and waveforms were recorded on a computer-controlled data acquisition system every 1 second to enable exact temporal correlation of the load and seismic response of the sample. The received waveforms consisted of 10,000 points representing a 100 microsecond window of the transmitted and reflected signals containing the compressional and shear waves.

Wavelet analysis was performed on all of the received signals to investigate changes in the amplitude and arrival time of the compressional and shear waves, and also the appearance of conversion S-to-P waves.

3. RESULTS

During loading, about 2800 images of the specimen surface were obtained but only 330 images were selected for the DIC analysis to obtain displacement and strain fields on the ROI; these included the period from crack initiation to coalescence and final failure. The DIC images were analyzed using the Vic-2D software licensed by Correlated Solutions. Details of the DIC analysis are presented in previous publications (Modiriasari et al., 2015 and 2016). The criterion to determine that a new crack formed required a discontinuity of magnitude 5 microns in the horizontal displacement between two adjacent points. This "jump" was chosen as the threshold value since it was small enough such that the position of the new crack tips could be determined and was larger than the noise in the DIC data.

The locations of new cracks at key loads, as well as the magnitude of the horizontal displacement discontinuities along the new cracks are presented in Fig. 3.

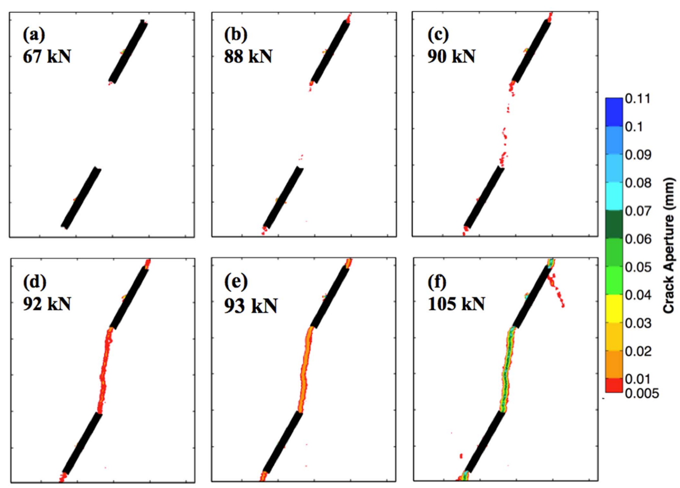

Fig. 3. Identification of new cracks and horizontal displacement discontinuities along new cracks obtained from DIC, at different loads.

Fig. 3a corresponds to a load of 67 kN where no new cracks had occurred. Fig. 3b shows the instant of appearance of the first shear cracks at the internal tips of the flaws, at 88 kN. Fig. 3c presents the propagation of the shear crack between the flaws, which was roughly parallel to the loading direction, at 90 kN. In Fig. 3d, the

DIC results show that crack coalescence occurred at 92 kN. Shear crack opening after crack coalescence is observed at 93 kN (Fig. 3e) and at failure, at 105 kN (Fig. 3f).

The transmitted and reflected signals were recorded during the entire test. Fig. 4 shows the transmitted and reflected signals from transducer 3S (this is the transducer placed between the two flaws and intended to monitor crack coalescence; see Fig. 2) as a function of load. Fig. 4a shows a 14-microsecond window of 10 of the 720 received transmitted shear waves collected during loading, from the initial load after honey coupling, to failure. The arrival time of the transmitted shear waves was approximately 42 μs, as shown in the highlighted area in Fig. 4a. The transmitted shear wave was delayed 1.07 μs and the amplitude of the signals attenuated (~30%) with increasing load up to crack coalescence at 92 kN. This continuous increase in the arrival time and decrease in amplitude of the transmitted waves started from the initial load, prior to the initiation of any cracks detected with DIC. This can be attributed to the gradual increase of micro-cracks inside the rock during compression.

Fig. 4b shows the transmitted signals between 30-40 μs, which is the time interval between the arrival time of P- (at ~25 μs) and S-waves (at ~42 μs). As observed in the highlighted region of Fig. 4b, for loads larger than 67 kN, another seismic wave with an arrival time of about 34 μs appears. This emerging wave at 34 μs, between the arrival time of transmitted P and S waves, is a wave conversion from the shear wave source transducer 3S to a compressional wave (S-to-P wave conversion). Based on the arrival time, the conversion occurs at the location of the growing shear crack. The amplitude of this signal increases with increasing load, up to crack coalescence. The reflected signals from transducer 3S, at different loads, are shown in Fig. 4c. The data are shown in a 10-microsecond window, with a highlighted area that includes the arrival time of the signals reflected from the new shear crack between the flaws. For a load of 105 kN (Fig. 4a-4c), the amplitude of the reflected signals increased immediately after crack coalescence, while the transmitted S-to-S and converted S-to-P waves decreased in amplitude.

4. DISCUSSION

A wavelet analysis was performed to examine the amplitude and arrival time of the signals. Previous findings using the displacement discontinuity theory suggested that changes in fracture properties could be better interpreted, at laboratory frequencies, using wave attenuation than wave velocity (Pyrak-Nolte et al., 2016). The measurements in the laboratory are often made using signals with a central frequency of 1 MHz on samples with length 10-15 times the wavelength (λ).

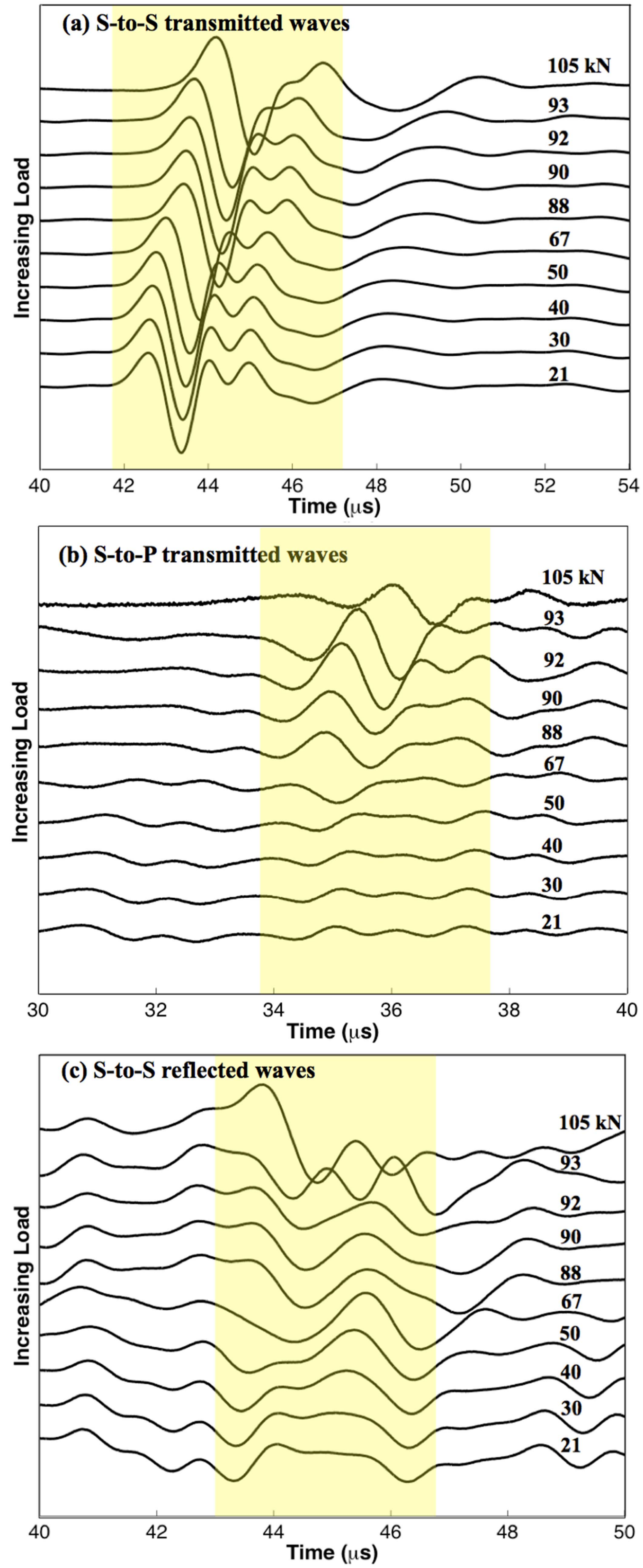

Fig. 4. Waveforms of transmitted and reflected signals from transducer 3S, with loading. (a) Wave transmission (S-to-S); (b) Wave conversion (S-to-P); (c) Wave reflection (S-to-S), represented in the highlighted areas.

Within this range, the maximum time delay caused by a fracture is about 8% of the time delay that results from propagating a wave over λ in the intact portion of the rock. The changes in time delays are relatively small compared to changes in amplitude of transmitted and reflected waves. Consequently, the changes in amplitude are easily measured at the laboratory frequencies and can be used to estimate fracture specific stiffness (Pyrak-Nolte et al., 2016). In this study, changes in amplitude of the signals were monitored to detect incipient damage and its evolution with load.

Fig. 5 shows the changes in normalized amplitude of the transmitted shear wave, converted S-to-P wave, and reflected shear wave as a function of load. All the amplitudes are normalized with respect to the amplitude of the transmitted shear wave (with a frequency of 440 kHz) through the intact sample between the flaws, at the initial compression of 2 MPa after honey coupling. The amplitude of the transmitted wave (represented by circles) decreases with increasing load, as explained in section 3. When shear crack initiation occurred between the two flaws, at 88 kN (Fig. 3b), the transmitted shear waves did not change significantly. This observation confirms our previous findings (Modiriasari et al. 2015) that show that transmitted waves are not sensitive to shear crack initiation. The reason is that when a shear crack initiates, the two fracture surfaces are largely in contact and shear displacements and dilation along the crack are not significant enough to be detected.

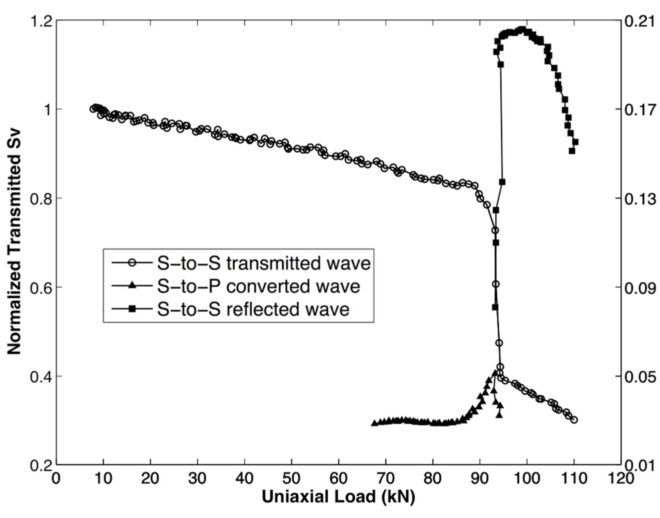

Fig. 5. Normalized amplitude of transmitted shear wave (S-to-S), converted wave (S-to-P), and reflected shear wave (S-to-S) from transducer 3S, with loading.

The seismic probe shows a sudden decrease (~50%) in amplitude of transmitted waves at a load of approximately 92 kN. The DIC results indicate that crack coalescence occurred at this time. At coalescence, the shear cracks reach a significant length, when enough shear displacements and dilation occurred to be detected. The crack opening at crack coalescence is very large as well, more than 10 microns, which causes a significant decrease in the stiffness of the shear crack and consequently in the amplitude of the transmitted shear waves.

An important finding is that, as load increased to approximately 67 kN, a converted mode (S-to-P wave) with an arrival time of ~34 μs emerged in the transmitted signals. The normalized amplitude of the converted waves is shown in Fig. 5 by the solid triangle symbols. This seismic signature was observed at roughly 76% of the shear crack initiation load detected with DIC imaging. This suggests that before a shear fracture can be detected on the specimen surface, internal damage inside the rock has already occurred, perhaps in the form of an array of oriented micro-cracks that induces partitioning of the energy from the S-wave into a P-wave. This is in agreement with previous findings by Nakagawa et al. (2000), who examined numerically and observed experimentally wave conversions along partially closed or frictional cracks, even for cases when a wave was normally incident to a fracture. They suggested that wave conversions were associated with fracture dilation when subjected to shear and normal stresses. As dilation occurs, the normal and shear stress on the fracture results in shear and normal displacements, respectively. They defined the coupling stiffness of the fracture as the normal or shear displacements resulting from the shear or normal stress, respectively, acting on the fracture. The local fracture stiffness increases along the approaching contacts and releases along the relaxed contacts between the two fracture surfaces. In this condition, an array of open flat inclined cracks exists along the fracture interface. The P- or S-waves normally incident on the array of oriented cracks partially convert to S- or P-waves, respectively. The converted waves are generated to a varying degree depending on the magnitude of the fracture dilation. This means as the coupling stiffness along the fracture interface increases, the conversion of waves increases. We hypothesize that before a macroscopic shear crack forms, an array of oriented micro-cracks is generated inside the rock. Consequently, the S-waves normally incident to the plane of micro-cracks partially convert to P-waves.

At loads larger than 88 kN, the load when the shear crack was detected with DIC, perhaps the micro-cracks grew and a macroscopic shear crack formed, which was associated with an increase in the amplitude of the converted wave by ~80%, just prior to crack coalescence. The amplitude of the converted waves approached a maximum at crack coalescence, i.e. at 92 kN, and was followed by a decrease after coalescence. The decrease in amplitude of the converted wave occurred because of the opening of the shear crack (more than 10 microns, as shown in Fig. 3e and 3f), i.e. loss of contact between the two shear crack surfaces.

The minimum in the amplitude of the transmitted and converted signals occurred at ~92 kN, which corresponded to the maximum of the normalized amplitude of the reflected waves (as represented by the solid square symbols in Fig. 5). After crack coalescence, when the two surfaces of the shear crack separated from each other, most of the energy of the seismic shear waves was reflected from the shear crack surface. As shown in Fig. 5, the reflected waves gradually decreased in amplitude after 105 kN, although the shear crack was opening further with compression. This was due to interference of the shear waves reflecting from the other shear crack at the external tip of the top flaw (Fig. 3f). The location of the new cracks was determined from the arrival time of the wave reflecting from the new cracks, which is consistent with previous findings (Modiriasari et al., 2015). As mentioned earlier, the experimental results presented here are consistent with those obtained from four other experiments on pre-cracked Indiana limestone samples with the same geometry, which brings confidence to the findings.

5. SUMMARY

The results presented are representative of those obtained from of an on-going experimental study on pre-cracked Indiana limestone specimens, to explore wave propagation as a tool to detect damage inside rock. Specimens with two parallel cracks are loaded until failure. Observations from the experiments include the detection of new cracks on the specimen surface using DIC as well as full waveforms of transmitted and reflected S-waves as well as converted S-to-P waves. In the experiments, coalescence occurs through a shear crack that links the internal tips of the flaws such that the coalescence crack is roughly parallel to the loading direction, and thus perpendicular to the incident S waves.

The results, albeit still preliminary, clearly show that changes in the amplitude of seismic waves propagated through rock can be used to detect the location, the time of initiation of shear cracks, as well as observe the evolution and coalescence of pre-existing flaws. The work presented in this paper complements earlier findings (Modiriasari et al., 2015) that indicated that the initiation of tensile cracks could be effectively detected by monitoring the changes of amplitude of the waves transmitted through the crack and its location by the arrival time of waves reflected from the crack. The past research also suggested that shear cracks could not be readily detected by transmitted waves unless the crack had significant slip and opening (dilation) deformations. Ongoing research on converted waves, part of which is presented in this paper, suggests that crack initiation and propagation of shear cracks can be detected by monitoring S-to-P wave conversion. Similar to previous findings regarding detection of tensile cracks with transmitted and/or reflected waves, changes of amplitude of the converted waves occur before the crack can be seen on the specimen surface using DIC. In other words, changes in amplitude of the converted waves can be used as precursors to rock damage in shear. The wave conversions are a signature of the partitioning of the wave energy that is incident to a shear crack. Because this signature is observed prior to shear crack detection on the specimen surface, it suggests the presence of incipient converted modes associated with an organized network of micro-cracks inside the rock. During compression, the micro-cracks grow. This is associated with an increase in the amplitude of the converted waves, until a macroscopic shear crack propagates and forms the coalescence crack. The coalescence is associated with a decrease in the amplitude of the waves transmitted through the crack and of the converted waves, and with an increase in the amplitude of the reflected waves.

The results of this experimental study show that active seismic wave monitoring has the potential to detect damage inside rock, at least at the laboratory scale.

ACKNOWLEDGMENTS

This research has been supported by the National Science Foundation, Geomechanics and Geotechnical Systems Program (award No. CMMI-1162082). The authors are grateful for this support.

REFERENCES

1. Pyrak-Nolte, L.J., L.R. Myer, and N.G.W. Cook. 1990. Transmission of seismic waves across single natural fractures. *Journal of Geophysical Research, 95(B6), 8617-38.*
2. Chen, W.Y., C. W. Lovell, G. M. Haley, and L. J. Pyrak-Nolte. 1993. Variation of shear-wave amplitude during frictional sliding. *International Journal of Rock Mechanics and Mining Sciences & Geomechanics Abstracts*, *30*(7), *779–784.*
3. Pyrak-Nolte, L.J. 1996. The seismic response of fractures and the interrelations among fracture properties. *International Journal of Rock Mechanics and Mining Sciences and Geomechanics Abstracts 33 (8): 787-802.*, *8*(33), *787–802.*
4. Nakagawa, S., K.T.T. Nihei, and L.R.R. Myer. 2000. Shear-induced conversion of seismic waves across single fractures. *International Journal of Rock Mechanics and Mining Sciences*, *37*, *203–218.*
5. Kahraman, S. 2002. The effects of fracture roughness on P-wave velocity. *Engineering Geology*, *63*(3–4), *347–350.*
6. Leucci, G., and L. De Giorgi. 2006. Experimental studies on the effects of fracture on the P and S wave

velocity propagation in sedimentary rock ("Calcarenite del Salento"). *Engineering Geology*, *84*(3–4), *130–142.*

7. Shao, S., and L. J. Pyrak-Nolte. 2013. Interface waves along fractures in anisotropic media, *GEOPHYSICS*, *78*(4*), T99–T112.*

8. Byun, J.H., J.S. Lee, K. Park, and H.K. Yoon. 2015. Prediction of crack density in porous-cracked rocks from elastic wave velocities. *Journal of Applied Geophysics*, *115*, *110–119.*

9. Modiriasri, A., A. Bobet, and L.J. Pyrak-Nolte. 2015. Monitoring of mechanically induced damage in rock using transmission and reflection elastic waves. *49th U.S. Rock Mechanics/Geomechanics Symposium.*

10. Aki, K., M. Fehler, R. L. Aamodt, J. N. Albright, R. M. Potter, C. M. Pearson, and J. W. Tester. 1982. Interpretation of seismic data from hydraulic fracturing experiments at the Fenton Hill, New Mexico, hot dry rock geothermal site, *Journal of Geophysical Research: Solid Earth, 87(B2), 936–944.*

11. Gu, B., R. Suarez-Rivera, K.T. Nihei, and L.R. Myer. 1996. Incidence of plane waves upon a fracture. *J. Geophysical Research: Solid Earth, 101(B11), 25,337–25,346.*

12. Nakagawa, S. 1998. Acoustic resonance Characteristics of rock and concrete containing fractures, *University of California, Berkeley.*

13. Modiriasri, A., A. Bobet, and L.J. Pyrak-Nolte. 2016. Monitoring rock damage caused by cyclic loading using seismic wave transmission and reflection. *50th U.S. Rock Mechanics/Geomechanics Symposium.*

14. Pyrak-Nolte, L.J., S. Shao, B.C. Abell. 2016. Elastic waves in fractured isotropic and anisotropic media. *To appear in CRC Volume Rock Mechanics and Engineering, edited Xia-Ting Feng.*